

Published in final edited form as:

J Am Chem Soc. 2008 October 1; 130(39): 12856–12857. doi:10.1021/ja804517m.

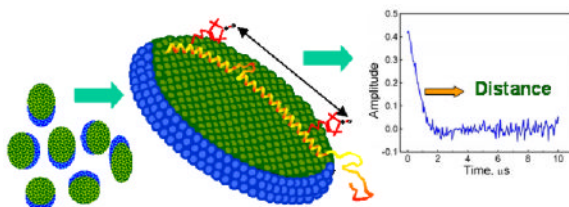
Membrane-Bound Alpha-Synuclein Forms an Extended Helix: Long-Distance Pulsed ESR Measurements Using Vesicles, Bicelles, and Rod-Like Micelles

Elka R. Georgieva[†], Trudy F. Ramlall[‡], Peter P. Borbat[†], Jack H. Freed[†], and David Eliezer[‡]

[†] Department of Chemistry and Chemical Biology, Cornell University, Ithaca, NY 14853

[‡] Department of Biochemistry and Program in Structural Biology, Weill Cornell Medical College, 1300 York Avenue, New York, NY 10065

Abstract



We apply pulsed dipolar ESR spectroscopy (Ku-band DEER) to elucidate the global conformation of the Parkinson's disease-associated protein, alpha-synuclein (α S) bound to small unilamellar phospholipid vesicles, rod-like SDS micelles, or lipid bicelles. By measuring distances as long as ~ 7 nm between introduced pairs of nitroxide spin labels, we show that distances are close to the expectations for a single continuous helix in all cases studied. In particular, we find distances of 7.5 nm between sites 24 and 72; 5.5 nm between sites 24 and 61; and 2 nm between sites 35 and 50. We conclude that α S does not retain a 'hairpin' structure with two antiparallel helices, as is known to occur with spheroidal micelles, in agreement with our earlier finding that the protein's geometry is determined by the surface topology rather than being constrained by the inter-helix linker. While the possibility of local helix discontinuities in the structure of membrane-bound α S remains, our data are more consistent with one intact helix. Importantly, we demonstrate that bicelles produce very similar results to liposomes, while offering a major improvement in experimentally accessible distance range and resolution, and thus are an excellent lipid membrane mimetic for the purpose of pulse dipolar ESR spectroscopy.

Alpha-synuclein (α S) was originally discovered as a protein highly enriched in synaptosome preparations from the electric ray *T. californica*¹ and was later linked to both familial and sporadic Parkinson's disease (PD) through the discovery that α S point mutations or gene duplication/triplication cause familial PD and through the identification of α S as the major component of amyloid fibril aggregates present in the Lewy body deposits that are a diagnostic hallmark of PD. Both the normal function of α S and the precise relation between its aggregation and deposition in Lewy bodies and PD remain unclear. When isolated in solution, the protein is intrinsically disordered, but in the presence of lipid surfaces α S adopts a highly helical structure² that is believed to mediate its normal function(s). NMR-based characterization of this helical structure using detergent micelles as a membrane mimetic has shown that the protein

adopts two extended surface-bound helices separated by a non-helical linker, that the helices are oriented in an antiparallel fashion, and that no inter-helical contacts are formed.^{3–7} The slow tumbling rate of intact phospholipid vesicles precluded direct studies of the vesicle-bound conformation of α S using solution NMR methods, but it was proposed^{3,8} that in the vesicle-bound state, the two helices may become collinear and fuse into a single long surface-bound helix. Support for this possibility was provided by pulsed dipolar ESR (PDS) distance measurements of α S bound to different sized micelles, which showed that the helices splay further apart on the surface of larger micelles.⁹

Here we use PDS,^{10–13} namely 17.3 GHz DEER (cf. Supplement), to measure distances in α S bound to lipid vesicles, rod-like micelles, and isotropic lipid bicelles, all of which present the protein with a more extensive, less highly curved surface than spheroidal micelles. Although it is possible to utilize a typical network of distances in the range of 2–4 nm, it is not prudent to draw conclusions about the global conformation and flexibility of a potentially ~14 nm long helix given uncertain nitroxide side-chain geometries. Therefore, our primary objective was to obtain long distance constraints. Although we obtain interpretable data using vesicle-bound synuclein, the signal to noise ratio is limited by the low average protein concentration that results from the small lipid surface area in a liposome sample and the need to use high lipid-to-protein molar ratios ($\sim 10^3$) to avoid lateral aggregation. Rod-like detergent micelles provide higher quality data, but do not represent a true lipid-bilayer environment. To circumvent problems associated with vesicles and micelles, we develop the use of PDS with lipid bicelles, which provide a true lipid-bilayer structure, yet have a particle size nearly as small as that of micelles and insure high lipid concentration and bilayer surface area. Bicelles have been successfully employed in solid state NMR experiments on membrane proteins, as well as to form liquid crystalline media for aligning proteins in solution.¹⁴ We show here that bicelles are also an attractive potential membrane mimetic for ESR studies of lipid-associated proteins. Fig. 1 and the supplement demonstrate the high quality data that can be obtained using lipid bicelles: comparable to or exceeding those obtainable using micelles and considerably superior to those obtained in the presence of vesicles. Distances measured for α S between labels placed from 15 to 48 residues (Fig. 1) apart are shown in Table 1. Labels at positions 24 and 61, located 37 residues apart and on opposite sides of the previously delineated linker region, yield distances of ~5.5 nm in the presence of all three types of particles. (For comparison, distances of ca. 4 nm were observed using these label positions in the presence of spheroidal micelles).⁹ This distance is in close agreement with that expected for a single continuous helix from position 24 to 61 (5.6 nm), but this agreement could be fortuitous, since several geometries involving two separated helices that are not collinear could result in such a distance. However, with labels at positions 24 and 72, an additional 11 residues apart, the distance in the presence of bicelles or rod-like micelles increases by 1.5 nm to ~7 nm. This increase in distance closely matches that expected for a continuous helical conformation (cf. Table 1). In fact, the average distance per residue (cf. Table 1) is within $\pm 1\%$ of that for an α -helix, which argues strongly for a single, unbroken helix as depicted in Fig. 2.

Measurements using spin-labeled E13C/H50C (~5 nm) and V3C/H50C (~6.5 nm) α S mutants further support the argument above. These distances are clearly too large for a ‘hairpin’ conformation but consistent with a highly extended structure. It is also notable that shorter distances between residues positioned closer to the linker (E35C/H50C), or having one of the residues within the linker (E20C/S42C and S42C/E61C), are also close to those expected for an α -helical structure. A control measurement using positions 50/72 that do not span the linker region also yields self-consistent results.

Previous ESR measurements of the environment of single spin labels attached to α S suggested that the region forming the linker in the micelle-bound conformation might be helical when the protein is bound to vesicles, in agreement with our explicit distance measurements.⁸ In

contrast, recent CW-ESR measurements of shorter distances between residues on opposite sides of the linker region were interpreted as indicating that the vesicle-bound protein also forms the broken helix 'hairpin'.¹⁵ Close inspection of the latter data, however, suggests that the measured distances may in fact be more consistent with an extended helical conformation than a broken helix for both the vesicle and micelle-bound protein. In addition, the range of distances from 1.4 to 1.8 nm is difficult to access by CW-ESR,¹⁶ whereas multiple studies have shown that long-distance constraints from PDS faithfully report on structures.^{17–20}

The natural binding target of α S in vivo is thought to be the surface of synaptic vesicles,^{3–8} the topology of which is most closely approximated in vitro by synthetic lipid vesicles. Thus, our results here suggest that when bound to synaptic vesicles in vivo, it is the extended helix conformation of α S that predominates. Nevertheless, several observations suggest that the broken-helix conformation observed in the presence of spheroidal micelles may also be relevant. Firstly, the distance distributions we observe are somewhat broader for inter-helix (i.e. between N and C helices, cf. Fig 2) than for intra-helix measurements, which may result from occasional bending or breaking of the helix (adding shorter distances to the distribution) and from conformations where the helix is partially unraveled (adding longer distances). Furthermore, measurements for a number of samples yielded somewhat bimodal distance distributions (cf. Supplement), which could result from distinct conformations of the protein, although this remains to be confirmed. These observations are consistent with the idea, also supported by a recent thermodynamic study of α S,²¹ that the protein can interconvert between the broken and extended helical forms.

α S binding to synaptic vesicles is considered to be weak, both based on in vitro measurements,^{22,23} and based on the fact that α S is observed to be largely cytoplasmic and mobile at synapses²⁴ and does not efficiently co-purify with synaptic vesicles. It is likely that the extended helix conformation exhibits this relatively low lipid affinity, possibly due in part to the unusual sequence periodicity of α S.^{3,8} In contrast, the broken helix form of α S binds to small micelles more tightly and has recently been postulated²⁵ to function in bridging two different membranes such as the synaptic vesicle and plasma membranes in the context of docked vesicles. Additional work is needed to further clarify the nature and mode of α S interactions with synaptic vesicles and other membranes, and PDS may prove to be helpful in this regard.

Supplementary Material

Refer to Web version on PubMed Central for supplementary material.

Acknowledgements

The authors thank Jaya Bhatnagar and Brian D. Zoltowski for help with CD and Gerald Feigenson, MingTao Ge, and Boris Dzikovski for useful discussions. Access to the Cornell NBTC facility is appreciated. This work was supported by grants NIH/NIA AG019391 and AG025440 (to D.E.), NIH/NCRR P41-RR016292 and NIH/NIBIB EB03150 (to J.H.F.) and by the Irma T. Hirschl Foundation and a gift from Herbert and Ann Siegel (to D.E.).

References

1. Maroteaux L, Campanelli JT, Scheller RH. *J Neurosci* 1988;8:2804–15. [PubMed: 3411354]
2. Eliezer D, Kutluay E, Bussell R Jr, Browne G. *J Mol Biol* 2001;307:1061–73. [PubMed: 11286556]
3. Bussell R Jr, Eliezer D. *J Mol Biol* 2003;329:763–78. [PubMed: 12787676]
4. Chandra S, Chen X, Rizo J, Jahn R, Sudhof TC. *J Biol Chem* 2003;278:15313–8. [PubMed: 12586824]
5. Bussell R Jr, Ramlall TF, Eliezer D. *Protein Sci* 2005;14:862–72. [PubMed: 15741347]
6. Ulmer TS, Bax A, Cole NB, Nussbaum RL. *J Biol Chem* 2005;280:9595–603. [PubMed: 15615727]
7. Bisaglia M, Tessari I, Pinato L, Bellanda M, Giraud S, Fasano M, Bergantino E, Bubacco L, Mammi S. *Biochemistry* 2005;44:329–339. [PubMed: 15628875]

8. Jao CC, Der-Sarkissian A, Chen J, Langen R. *Proc Natl Acad Sci USA* 2004;101:8331–36. [PubMed: 15155902]
9. Borbat P, Ramlall TF, Freed JH, Eliezer DJ. *Am Chem Soc* 2006;128:10004–5.
10. Berliner, L.J.; Eaton, GR.; Eaton, SS., editors. *Biological Magnetic Resonance*. 21. Kluwer-Plenum; NY: 2000.
11. Borbat PP, Freed JH. *Methods in Enzymology* 2007;423:52–116. [PubMed: 17609127]
12. Jeschke G, Polyhach Y. *Phys Chem Chem Phys* 2007;9:1895–910. [PubMed: 17431518]
13. Schiemann O, Prisner TF. *Quarterly Rev Biophys* 2007;40:1–53.
14. Prosser RS, Evanics F, Kitevski JL, Al-Abdul-Wahid MS. *Biochemistry* 2006;45:8453–65. [PubMed: 16834319]
15. Bortolus M, Tombolato F, Tessari I, Bisaglia M, Mammi S, Bubacco L, Ferrarini A, Maniero AL. *J Am Chem Soc* 2008;130:6690–1. [PubMed: 18457394]
16. Banham JE, Baker CM, Ceola S, Day IJ, Grant GH, Groenen EJJ, Rodgers CT, Jeschke G, Timmel CR. *J Magn Reson* 2008;191:202–8. [PubMed: 18280189]
17. Borbat PP, Mchaourab HS, Freed JH. *J Am Chem Soc* 2002;124:5304–14. [PubMed: 11996571]
18. Borbat PP, Surendhran K, Bortolus M, Zou P, Freed JH, McHaourab HS. *PLoS Biol* 2007;5:2211–9.
19. Park SY, Borbat PP, Gonzalez-Bonet G, Bhatnagar J, Pollard AM, Freed JH, Bilwes AM, Crane BR. *Nat Struct Mol Biol* 2006;13:400–7. [PubMed: 16622408]
20. Fafarman AT, Borbat PP, Freed JH, Kirshenbaum K. *Chem Commun* 2007:377–9.
21. Ferreon AC, Deniz AA. *Biochemistry* 2007;46:4499–509. [PubMed: 17378587]
22. Bussell R Jr, Eliezer D. *Biochemistry* 2004;43:4810–8. [PubMed: 15096050]
23. Rhoades E, Ramlall TF, Webb WW, Eliezer D. *Biophys J* 2006;90:4692–700. [PubMed: 16581836]
24. Fortin DL, Nemani VM, Voglmaier SM, Anthony MD, Ryan TA, Edwards RH. *J Neurosci* 2005;25:10913–21. [PubMed: 16306404]
25. Eliezer, D. Parkinson's Disease. In: Nash, R.; Przedborski, S., editors. *Pathogenic and Therapeutic Insights from Toxin and Genetic Models*. Elsevier; 2008. p. 575-95.

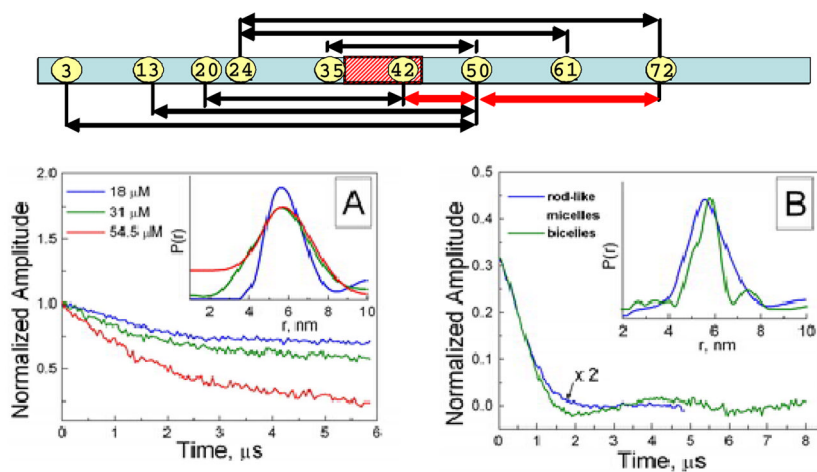


Figure 1. Top - Schematic illustrating the positions, within the lipid-binding domain of α S, of the spin-labeled sites used for distance measurements. Intra (inter) helix distances are shown in red (black) lines. Bottom - DEER signals for α S mutant Q24C/E61C in (A) POPC:POPA liposomes, (B) rod-like SDS micelles and bicelles.

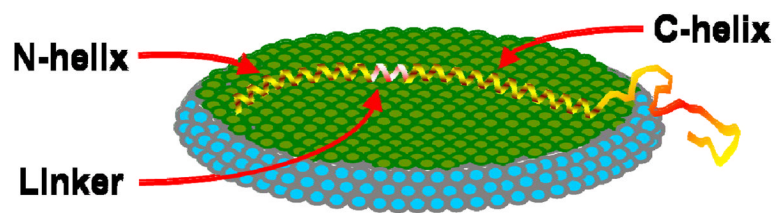


Figure 2.
Schematic model for the conformation of α S bound to the lipid bilayer of a bicelle based on ESR distance measurements.

Table 1
Pulse dipolar ESR distance measurements on α S bound to liposomes, bicelles, and rod-like SDS micelles.^a

Labeled Sites	α -Helix		Bicelles		Liposomes		Rod-Like Micelles	
	R	ΔR	R	ΔR	R	ΔR	R	ΔR
24/61	5.6	1.2	5.8	1.2	5.5 ^b	2.1	5.5	1.7
24/72	7.2	1.9	7.5	1.9	5.6 ^c	2.3	6.9	1.0
13/50	5.6	1.3	5.3	1.3	5.1 ^b	2.7	5.0	1.7
3/50	7.1	2.5	6.3	2.5	-	-	6.7	1.4
20/42	3.3	1.3	3.3	1.3	3.3 ^b	1.3	3.3	1.3
35/50	2.3	0.7	2.0	0.7	2.0 ^c	0.7	-	-
42/61	2.9	1.0	3.6 ^d	1.0	3.6 ^b	0.8	3.6	1.1
50/72	3.3	0.9	3.8	0.9	3.5 ^c	0.8	-	-
Helix Rise	0.15			0.152 ^e				0.148 ^e

All distances (R) and distribution widths (ΔR) were rounded to 0.1 nm.

^a Site labeling shown in Fig. 1 and in Ref. 9.

^b DMPC:DMPG (1:1);

^c POPC:POPA (1:1);

^d There is also a weaker narrow peak at 2.9 nm. (cf. Supplement)

^e Average spin-label separation per residue (nm).